International Journal of Technology

http://ijtech.eng.ui.ac.id

Research Article

Utilization of E-Waste Plastic-Coated Recycled Aggregates in Concrete: A Sustainable Waste Management and Construction Innovation Solution

J. Rajprasad[1*], Musa Adamu[2], M. Mohamed Ajmal[1], Yasser E. Ibrahim[2]**

[1]Department of Civil Engineering, College of Engineering and Technology, SRM Institute of Science and Technology, Kattankulathur, 603203, Tamil Nadu, India

[2]Engineering Management Department, College of Engineering, Prince Sultan University, 11586 Riyadh, Saudi Arabia

[*]Corresponding author: rajprasj@srmist.edu.in,

[**]Corresponding author: madamu@psu.edu.sa,

Abstract: This study evaluates the use of e-waste plastic powder as a surface coating for recycled concrete aggregate (RCA) to mitigate the strength and durability penalties associated with RCA in M30 concrete. RCA was coated at an RCA-to-powder ratio of 6:1 and used to replace natural coarse aggregate at 15%, 20%, and 25% (ECRA series), alongside a control mix and uncoated RCA mixes, with a constant water-to-cement ratio (w/c) of 0.43. Mechanical performance was assessed at 7, 14, and 28 days using compressive, splitting tensile, and flexural strength tests, while durability was evaluated by 5% hydrochloric acid (HCl) exposure, 5% sodium sulfate (Na_2SO_4) exposure, water absorption, and the rapid chloride permeability test (RCPT). Supporting characterization included X-ray diffraction (XRD), Fourier transform infrared spectroscopy, scanning electron microscopy (SEM), thermogravimetric analysis (TGA), and differential thermal analysis (DTA). At 28 days, 20% ECRA achieved a compressive strength of 31.98 MPa, comparable to that of the control (32.17 MPa), whereas 20% uncoated RCA reduced the compressive strength by 11%. The splitting tensile strength increased to 3.42 MPa at 20% ECRA (vs. 3.35 MPa control), and the flexural strength improved by 1.92%. Durability also improved: 28-day water absorption decreased to 6.4% for 20% ECRA (vs. 7.5% for 20% RCA) and RCPT charge reduced to 245–658 C for ECRA mixes (vs. 1058 C for the control). TGA indicated only 4.02% mass loss up to 700 °C, indicating good thermal stability. Overall, e-waste powder coating enhanced the performance of recycled aggregate concrete, with 20% ECRA providing the best balance of mechanical and durability behavior.

Keywords: Coated recycled aggregate; E-waste powder; Electronic waste; Recycled aggregate

1. Introduction

The building industry is essential to the global economy but significantly contributes to environmental degradation, resource depletion, and waste generation (Kuzina et al., 2018). Because sustainable resource management is increasingly required, eco-friendly construction materials are gaining attention (Abrahams, 2017). One major approach is to use recycled aggregate (RA) in concrete, which reduces the demand for virgin aggregate and diverts construction and demolition waste from landfills (Wang et al., 2021). RA can be produced from demolished structures, industrial debris, and construction leftovers, helping preserve natural resources and support circular-economy goals by minimizing raw material use and waste (de Andrade Salgado and de Andrade Silva, 2022; Agrawal et al., 2021; Mangialardo and Micelli, 2017;Gulghane and Khandve, 2015;Faniran and Caban, 1998).

However, the wider structural use of recycled aggregate concrete (RAC) is limited because RA often reduces mechanical performance due to adhered mortar, higher porosity, and greater

https://doi.org/10.14716/ijtech.v17i2.8027
Received August 2025; Revised November 2025; Accepted February 2026

water absorption (de Andrade Salgado and de Andrade Silva, 2022; Gulghane and Khandve, 2015). As a result, many studies have focused on improving RA/RCA quality through treatment methods such as washing, mortar removal, and pore modification, which generally improve strength compared to untreated aggregates, although performance reductions may still remain at high replacement levels (Sangamesha et al., 2023). Mix-design optimization and improved processing methods (including combining RCA with natural aggregates) have also been shown to stabilize RAC performance and enable higher replacement levels while maintaining acceptable mechanical properties (Bui et al., 2017; Lotfi et al., 2015). Since concrete must satisfy the requirements of strength, stability, and durability, achieving consistent performance remains central to expanding RAC applications (Shahane and Bhosale, 2021; Perkins et al., 2014).

In parallel, e-waste is a growing global problem due to toxic components and disposal challenges, but it also offers opportunities for reuse in construction materials (Luhar and Luhar, 2019; Mangialardo and Micelli, 2017; Perkins et al., 2014). Studies have reported that e-waste plastics can be technically and economically feasible as aggregates or fillers in pavements and concrete, with some evidence of improved strength at specific replacement ranges, and other research has combined e-waste with industrial by-products (e.g., steel slag) to enhance concrete properties (Bharani, Rameshkumar, et al., 2021; Muthupriya and Kumar, 2021; Needhidasan et al., 2020). Building on this sustainability pathway, e-waste powder coating (EWPC) has been proposed as a surface treatment method for recycled aggregates to improve their performance in concrete, potentially enhancing bonding and reducing the negative effects associated with adhered mortar and porosity (Lokesh Kumar et al., 2024; Raman and Ramasamy, 2021; Shahane and Bhosale, 2021). Finally, the reliability of established experimental datasets on RAC mechanical properties—compressive strength, splitting tensile strength, and elastic modulus—provides a strong foundation for evaluating whether EWPC-treated recycled aggregates can meet performance norms while delivering environmental benefits (Álvarez-Pérez et al., 2021; Wu et al., 2014; McNeil and Kang, 2013).

1.1 Sources of electronic waste (E-waste)

E-waste arises from various end-of-life electrical and electronic products. Televisions, refrigerators, washing machines, desktop and laptop computers, radios, mobile phones, cameras, modems, batteries, CRT-containing devices, and CD/DVD players are common examples (Marimuthu and Ramasamy, 2024; Niu et al., 2024; Janani et al., 2023; Masud et al., 2022; Roy et al., 2022; Ullah et al., 2022). The defined equipment categories are summarized in Table 1.

In addition, the Basel Convention classifies equipment as e-waste when its rated voltage does not exceed 1,500 V for direct current or 1,000 V for alternating current (Hino et al., 2009). Table 2 summarizes the typical material constituents of electrical and electronic equipment (WEEE), and Figure A1 presents a schematic flowchart outlining the main generation pathways and potential sources of e-waste in the Supplementary file.

Conventional WEEE streams include discarded computers, televisions, air conditioners, printers, washing machines, and refrigerators. These items are commonly grouped by application type, including: (i) large household appliances, (ii) small household appliances, (iii) telecommunications and IT equipment, (iv) lighting products, (v) consumer electronics, (vi) toys and sports equipment, (vii) automatic dispensers, (viii) medical devices, (ix) monitors, and (x) control instruments. Many of these products require formal recovery and recycling because they contain both hazardous substances and valuable recoverable materials, highlighting the need for structured e-waste management. E-waste typically contains mixtures of metals and metalloids, along with organic contaminants. The presence and concentrations of these constituents vary according to the device type and component composition. These materials are widely recognized as potential risks to human health and the environment (Szałatkiewicz, 2014; Yamane et al., 2011; Hino et al., 2009).

Table 1 Summary of the tools in the classifications

Categories	E-wastes
IT and telecommunications	IT and telecom equipment: PCs, laptops, copiers, calculators, printers, fax/telex units, user terminals, telephones, and other data/voice devices.
Small house appliances	Small household appliances: cleaning, garment/textile care, small kitchen tools, and personal-care devices.
Large house appliances	Large household appliances: cooking, heating, washing/drying, dishwashing, and cooling/storage equipment.
Consumer appliances	Consumer electronics: TVs, radios, cameras/recorders, hi-fi systems, musical gear, and other audio/video devices.
Lighting equipment	Lighting equipment: bulbs, fluorescent/energy-saving lamps, fixtures, traffic lights, and industrial lighting.
Electrical and electronic devices	Electrical/electronic tools: power tools for cutting/drilling/grinding, fastening, welding/spraying, and powered gardening tools.
Monitoring and instrument control	Monitoring and control instruments: thermostats, heating controllers, measuring/weighing devices, and industrial monitoring equipment.
Medical tools	Medical tools: laboratory analyzers, fertility testers, dialysis/cardiology devices, ventilators, and other diagnostic/treatment equipment.
Automatic dispensers	Automatic dispensers: drink machines, can/bottle vending units, and other dispensing machines.
Sports equipment and toys	Sports and toys equipment: electronic toys, gaming consoles/games, and sports devices (cycling, swimming, racing, rowing, etc.).

Table 2 Major WEEE items and their typical primary components

General WEEE	Typical Primary Components
Television	Internal wiring: Power/signal harnesses connecting the boards, controls, speakers, and display.
Computer	CPU unit, keyboard/mouse, battery, speakers, wiring, PCBs, and display unit (LCD and CRT)
Washing machine	Drive motor, drain hose, internal tubing, and wiring
Refrigerator	Condenser assembly, tubing/liners, refrigerant circuit, and wiring
Air conditioner	Compressor, fan motor, heat exchanger, refrigerant circuit, wiring, printed circuit board, copper piping
Duplicator / Printer	Toner and cartridge, rollers, printed circuit board, wiring

Recycled concrete aggregate (RCA) remains limited in higher-grade recycled aggregate concrete (RAC) because adhered mortar and surface porosity weaken the interfacial transition zone (ITZ), increase water absorption/permeability, and reduce strength and durability. In parallel, unmanaged electronic waste (e-waste) presents a disposal/toxicity concern due to hazardous constituents (e.g., cadmium, lead, and mercury), motivating controlled reuse pathways that reduce exposure risk while maintaining concrete performance. The technical gap is a scalable route that simultaneously improves RCA surface/ITZ quality and e-waste in a safe, performance-verified manner.

Current practice typically combines RCA pre-treatments (to reduce adhered mortar effects and modify pore structure), mix-design compensation (partial replacement, admixtures), and supplementary cementitious material (SCM) coatings intended to densify RCA surfaces and enhance ITZ bonding. In parallel, e-waste reuse in cementitious systems is advancing through filler/aggregate/additive concepts, increasingly supported by microstructural and physicochemical diagnostics (XRD/FTIR/SEM/TGA-DTA) to link observed performance to material interactions. Although these approaches reduce typical RCA penalties, their performance can remain sensitive to RCA variability and replacement level.

The document's approach e-waste powder-coated RCA (ECRA)—targets the root mechanism by densifying the RCA surface and strengthening the ITZ to reduce permeability indicators and recover mechanical performance. A key strength is the reported performance recovery at an optimum replacement (notably improved strength retention and durability indices such as water absorption/RCPT), with supporting microstructural/thermal evidence including XRD/FTIR/SEM and low mass loss in TGA up to 700 °C. A key weakness is non-monotonic behavior at higher replacement (reduced performance at 25%), indicating sensitivity to dosage and microstructural heterogeneity. The manuscript notes the need for long-term durability, structural element testing, LCA, and field validation for adoption.

A state-of-the-art extension is an "engineered RCA" concept using a functionally graded hybrid surface layer: (i) a thin mineral/reactive primer to fill surface-connected pores and strengthen the adhered mortar region (directly targeting RCA porosity/ITZ weakness), followed by (ii) a controlled e-waste powder micro-seal to reduce ingress pathways and enhance bonding (retaining the demonstrated ECRA mechanism). To ensure consistency and scalability, we implemented performance-based qualification aligned to the manuscript's indicators: permeability-first screening (water absorption + RCPT), microstructure verification (SEM/FTIR/XRD for coating continuity and ITZ improvement), and thermal screening (TGA/DTA to confirm limited thermally labile content). Then, we closed the adoption gap through long-term durability exposures, element-level structural behavior, LCA, and field trials.

This study investigates e-waste powder-coated recycled concrete aggregate (ECRA) to address the key limitations of recycled concrete aggregate (RCA), namely adhered mortar and surface porosity, which weaken aggregate-paste interlock, increase water absorption, and reduce strength and durability. Unlike conventional RCA improvement methods (pre-treatments or cementitious coatings), this study applies e-waste-derived powder as a surface coating to densify the RCA surface, strengthen the interfacial transition zone (ITZ), and reduce permeability. This study (i) compares conventional concrete with RCA concrete and (ii) evaluates whether ECRA mitigates typical RCA performance penalties. Mechanical performance was assessed via compressive, split tensile, and flexural strength, while durability was evaluated through acid and sulfate resistance, water absorption, and chloride ion penetration resistance. XRD, FTIR, SEM, and TGA/DTA are used to confirm coating presence, interactions, and microstructural effectiveness, supporting a sustainable route for co-utilization of e-waste and recycled aggregates.

1.2 Objectives of the research

This study aims to determine whether e-waste powder-coated recycled concrete aggregate (EWPC-RCA) can mitigate the typical strength and durability reductions associated with RCA in M30 concrete. Concrete mixes with 15%, 20%, and 25% replacement levels were produced and compared with conventional concrete. Compressive, splitting tensile, and flexural strength tests were used to evaluate performance, along with durability assessments, including acid resistance, sulfate resistance, water absorption, and chloride penetration resistance. Microstructural and thermal characterization (XRD, FTIR, SEM, and TGA/DTA) were used to support the interpretation of the observed behavior.

2. Materials and Methods

2.1 Materials

Concrete was produced using cement, fine aggregate, coarse aggregate, potable water, and chemical admixture in accordance with relevant Indian Standards. Ordinary Portland cement (OPC) grade 53 (Type I) with a specific gravity of 3.15 and fineness of 345 m^2/kg was used as the binder. Manufactured sand (M-sand) conforming to IS 383 (2016) was used as the fine aggregate; it had a maximum particle size of 4.75 mm and was classified as Zone II. The physical properties of the fine aggregate are reported in Table B1 in the Supplemental Material. Crushed granite natural stone was used as aggregate (NA) with a nominal maximum size of 12.5–20 mm was used, together with recycled concrete aggregate (RCA) and e-waste powder-coated RCA as alternative coarse aggregates. The properties of NA, RCA, and the e-waste plastic powder are summarized in the Supplementary file (Appendix A), while the chemical characteristics of the e-waste powder are presented in the Supplementary file (Table B2). To improve workability, a commercially available superplasticizer (Classic Crete Superflo-SP) conforming to IS 2645:2003 (specific gravity 1.24, chloride-free, 48% solids) was incorporated as a water-reducing admixture. Potable tap water (pH 6.5–7.0) that satisfies the IS 456:2000 requirements was used for mixing and curing. For EWPC-RCA preparation, RCA particles were coated with the prepared e-waste powder by thorough mixing to achieve uniform surface coverage; loose and excess powder was removed. The coated aggregates were then spread on a polythene sheet and sun-dried for seven days before incorporation in the concrete mixes. The complete coating and preparation procedure is illustrated in Figure A2 in the supplementary file.

2.2 Mix Proportioning

In this study, grade M30 concrete was designed in accordance with Bureau of Indian Standards, 2009 A mix ratio of 1:1.42:2.75 was used, and the water-cement ratio was maintained at 0.43 throughout the mixes. The recycled concrete was coated with E-waste plastic powder in a ratio of 1:6, i.e., 6 parts of recycled aggregate to 1 part of E-waste plastic powder. The natural coarse aggregate was replaced with recycled coarse aggregate in the following ratios: 15%, 20%, and 25%. In another mix series, the natural coarse aggregate was replaced with the E-Waste Coated Recycled Aggregates (ECRA) in proportions of 15%, 20%, and 25%. Table 3 shows the mix proportions and their constituent materials.

Table 3 Mix proportions (kg/m^3) for M30 control, RCA (15%-25%), and e-waste powder-coated RCA mixes (15-25%)

Mix ID	Cement (kg/m^3)	Fine aggregate (kg/m^3)	Coarse aggregate (kg/m^3)	Recycled coarse aggregate (kg/m^3)	E-Waste-coated aggregate (kg/m^3)	Water (kg/m^3)	W/C
CC	425.73	605	1172	-	-	197	0.43
RCA 15%	425.73	605	998.75	173.25	-	197	0.43
RCA 20%	425.73	605	937.6	234.4	-	197	0.43
RCA 25%	425.73	605	879	293	-	197	0.43
ECRA 15%	425.73	605	998.75	-	173.25	197	0.43
ECRA 20%	425.73	605	937.6	-	234.4	197	0.43
ECRA 25%	425.73	605	879	-	293	197	0.43
Mix ratio is 1:1.42:2.75:0.43							

2.3 Samples Preparation

Material preparation and batching procedures were carefully controlled to ensure consistency and reproducibility of the concrete mixes. Cement, M-sand, and coarse aggregates were oven-dried and spread in a tray to achieve uniform color, eliminate moisture, and prevent agglomeration. The constituent materials were weighed according to the mix design and initially dry-mixed to ensure homogeneity. Approximately 50% of the total mixing water was first added to the dry blend and thoroughly mixed. Subsequently, the superplasticizer was dissolved in 40% of the mixing water and introduced into the partially wetted mixture. The remaining 10% of water was gradually added during final mixing to achieve uniform consistency. Before casting, all molds were cleaned and coated with a thin layer of lubricant to facilitate demoulding. Fresh concrete was cast immediately after mixing, and workability (slump) and temperature were measured to ensure quality control. Compaction was carried out using a vibrating table to eliminate trapped air. After curing, the concrete specimens were tested for compressive, split tensile, and flexural strength according to the relevant standards. A 150-mm concrete cube was cast for compressive strength testing. For the splitting tensile strength test, cylindrical samples with 150 mm diameter and 300 mm height were cast. For the flexural strength test, prismatic samples with dimensions of 150 mm × 150 mm × 700 mm were cast. A total of 21 samples were cast and cured for the compressive, splitting tensile, and flexural strength tests for 7, 14, and 28 days before testing.

2.4 Pretreatment of electronic waste through shredding, grinding, milling, and sieving

The first step in e-waste recycling is WEEE pre-treatment, which is mainly used to liberate metallic and non-metallic components through physical operations such as dismantling, crushing/milling, screening, and separation. Recovery efforts increasingly focus on high-value metals (Au, Ag, Pd, Cu) and rare-earth-containing compounds, using physical separation, chemical methods, and hydro-/pyrometallurgical routes. Physical separation is the most common because it is low-cost and requires less capital. However, it can cause notable metal losses (about 15%–30%) and is a mature technology with limited further scale-up potential. Standard pretreatment stages include: (1) dismantling and de-soldering, (2) size reduction to fine particles, (3) screening (rotary/vibrating), and (4) separation into metallic fraction (MF) and non-metallic fraction (NMF). These steps also improve the efficiency of downstream recovery processes. In the described plastic aggregate-production sequence: plastic is shredded, screened to remove wiring, melted at $\tilde{2}00$ °C, quenched and solidified, and crushed to produce aggregates of the desired size (Figure 1).

The mechanical pretreatment of WEEE is typically implemented as a staged sequence of shredding, grinding, milling, and sieving to progressively increase the liberation of material. Shredding with low-speed, high-torque single/twin-shaft units reduces whole devices to coarse fragments ($\tilde{2}$0–100 mm) for safer handling and stable downstream feeding, but with limited liberation. Subsequent grinding in hammer mills, impact crushers, or granulators produces $\tilde{5}$–20 mm particles and improves liberation by exploiting brittle–ductile contrasts: ceramics/glass/solder fracture, while metals deform and detach from polymer matrices. For high recovery of embedded and precious metals (notably in PCBs), milling (ball/rod/attrition) generates fine material (<1 mm; typically $\tilde{7}$5–500 μm) suitable for efficient downstream separation, though it is energy-intensive and prone to over-grinding losses. Final sieving (vibratory/rotary) classifies size fractions, enabling coarse recycling for re-grinding and routing fines for physical or chemical separation. This integrated train controls liberation and particle-size distribution, directly affecting separation efficiency, selectivity, and process economics.

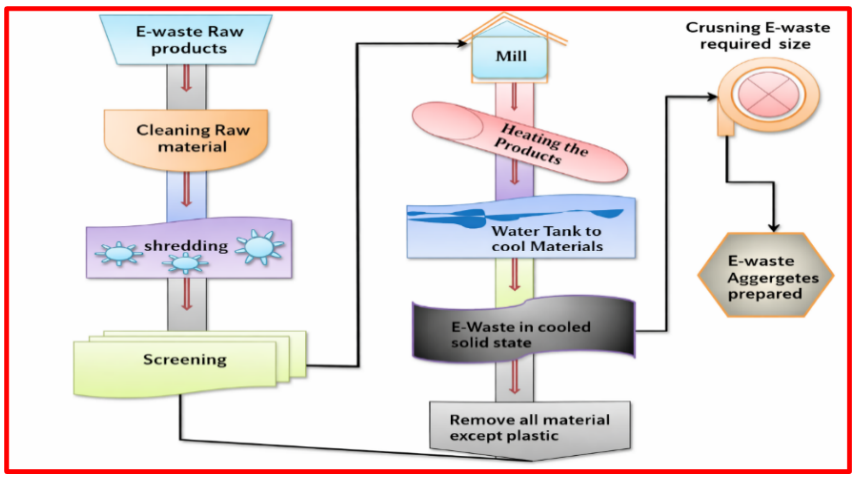

(a)

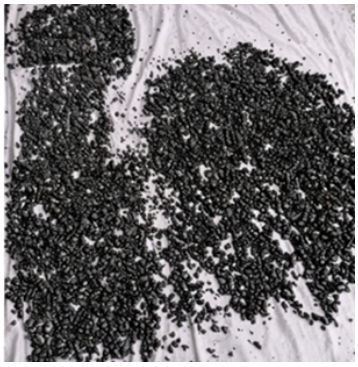

(b) (c) (d)

Figure 1 (a)Manufacturing process of plastic aggregates (b) Plastic rocks (c) Crushed state (d) Sieve analysis Different steps towards the production of E-waste powder

2.5 Mechanical strength testing

The Bureau of Indian Standards, 2021 test specification was used to test the compressive strength of conventional concrete (CC), recycled coarse aggregate concrete (RCA), and e-waste coarse aggregate concrete (ECRA) mixes. The 150 × 150 × 150 mm concrete test specimens were cured for 7, 14, and 28 days after removal from the molds before testing. The compression test was conducted using a 3000 kN capacity UTM.

The mechanical properties of hardened concrete were investigated through split tensile and flexural strength tests on CC, RCA, and ECRA. The split tensile strength was determined at curing ages of 7, 14, and 28 days in accordance with Bureau of Indian Standards, 1999. Slight variations in the water-cement ratio, constituent proportions, workability (slump), and curing conditions can significantly influence the strength development and structural stability of concrete.

M30 grade concrete incorporating e-waste as a partial replacement for coarse aggregate was prepared and tested at replacement levels of 15%, 20%, and 25%, respectively. Specimens were cured and evaluated at 7, 14, and 28 days to assess the effect of e-waste content on TP. Flexural strength tests for CC, RCA, and ECRA mixes were conducted at 7, 14, and 28 days in accordance with Bureau of Indian Standards, 2021. Bureau of Indian Standards, 2021 Prismatic beam specimens measuring 150 × 150 × 700 mm were used. The compressive, split tensile, and flexural strength tests for each specimen are shown in the Supplementary file as Figure A3. Three specimens were tested for each mechanical property for each mix proportion and test age, and the mean value was reported as the representative result.

2.6 Durability and strength testing

For the acid attack resistance test, the concrete was damaged by 5% HCl. These concrete mixtures had ECRA and CC substitutions of 15%, 20%, and 25% RCA. The specimens were immersed in HCl to simulate harsh environmental conditions and measure the resistance to acid attack based on mass loss and surface deterioration. ECRA-containing concrete survived CC and RCA. The ECRA specimens revealed low mass loss and surface degeneration after 7, 14, and 28 days of acid exposure. Acid attack was prevented by coating the RCA particles with plastic powder. A novel approach may improve the durability of recycled aggregate concrete (Xiao et al., 2025).

Water absorption checks the concrete permeability. Samples were analyzed after 24 h in water. Water absorption was measured by weight growth. Water absorption reflects the permeability of concrete to freeze-thaw cycles, chemical attack, and reinforcing corrosion. Predicting concrete construction durability requires understanding water absorption over time (Singh and Siddique, 2025). This study tested the water absorption of recycled CA-coated plastic powder concrete specimens under different environmental conditions. Concrete specimens with 15%, 20%, and 25% RCA substitution and 100% natural coarse aggregate control specimens were examined for water absorption at 7, 14, and 28 days.

RCPT measures concrete chloride ion (CI) resistance. Concrete voltage measurement for CI ion migration. This is crucial for assessing reinforced concrete construction durability in coastal and de-icing salt-exposed areas. Ions degrade steel reinforcement, thereby endangering the structural stability and safety of concrete. Building durable infrastructure requires an understanding of the movement of chloride ions in concrete. RA in concrete production is becoming popular for environmental and resource efficiency. Concrete durability and chloride ion permeability make RA integration challenging (Zhu et al., 2020). Concrete with 15%, 20%, and 25% RCA and ECRA partial CC replacement underwent RCPT. At 7, 14, and 28 days, these specimens and 100% NCA controls were tested for chloride ion penetration resistance using RCPT. Testing concrete for chloride ion mobility using voltage. The RCA/ECA concrete showed better chloride ion penetration resistance than the controls. Reduced chloride ion penetration has been demonstrated by lower RCA and ECRA electrical conductivities. Plastic powder coating improves the durability of recycled aggregate concrete by decreasing chloride ion penetration as RCA replacement increases.

Concrete becomes sulfate-sensitive when 15%, 20%, or 25% NCA is replaced with RCA and ECRA. Sulfate attack tests at 7, 14, and 28 days were performed using standard methods. To simulate aggressive sulfate-rich conditions, sulfate solutions were applied to concrete (Jabbour et al., 2022). The sulfate resistance of RCA and ECRA concrete varies depending on the replacement percentage and testing time. Durability reduced as RCA and ECRA substitution increased sulfate attack risk. Plastic powder-coated RCA reduces sulfate attack at higher replacement percentages and longer testing times. These findings indicate that PPC may increase sulfate resistance and recycled concrete durability.

2.7 Microstructural Evaluation

X-ray diffraction (XRD) and Fourier transform infrared spectroscopy (FTIR) were used to examine the ECRA structure. Scanning electron microscopy (SEM) was used to study e-waste assimilation into concrete and surface morphology. Thermogravimetric Analysis (TGA)/DTA was used to evaluate the thermal stability. These methods describe the crystalline structure, surface properties, and temperature resistance of the materials.

3. Results and Discussion

The M30 grade CC, RCA, and ECRA concrete mixes were evaluated for their compressive, split tensile, and flexural strengths. Three cubes, three cylinders, and three beams were evaluated for strength averages at 7, 14, and 28 days. The test results were examined.

3.1 Compression strength of the CC, RCA, and ECRA concrete samples

At 7, 14, and 28 days, the CC, RCA, and ECRA concrete compression strengths differ (Figure 2). After 7, 14, and 28 days, the CC compressive strengths were 16.88, 20.26, and 32.17 N/mm². RCA reduces the concrete compressive strength at 7, 14, and 28 days. 15% RCA replaces natural coarse aggregate after 28 days, reducing compressive strength by 7.33%. The 28-day reduction is 11% with 20% RCA and 17.74% with 25% RCA. The ITZ between the concrete paste and aggregate particles considerably affects the concrete strength. The ITZ may weaken with the recycling of aggregates, lowering the bond and compressive strength (Liu et al., 2022). ECRA enhanced the compressive strength of natural coarse aggregate. Aggregate coating increases compressive strength. This investigation confirmed earlier findings. Pozzolanic aggregate increases compressive strength, per Li et al., 2009. The concrete containing 20% E-waste-coated recycled aggregate had the highest compressive strength of 31.98 N/mm². Urban and Sicakova, 2017 reported 27.7 N/mm² compressive strength of fly-ash-coated RCA concrete. However, Sasanipour and Aslani, 2020 observed that silica fume coating of recycled coarse aggregate did not increase compressive strength. Comparing current studies (Olofinnade and Osoata, 2023; Urban and Sicakova, 2017; Li et al., 2009), e-waste as recycled aggregate coating was better than SCMs like silica fume, GGBS, and fly ash. Natural coarse aggregate was replaced with 15% ECRA, which enhanced compressive strength by 0.7%. The replacement of natural coarse aggregate concrete with 20% ECRA enhanced the compressive strength by 2.88%. ECRA may raise aggregate-concrete paste ITZ due to its surface. The compressive strength decreased slightly when 25% natural coarse aggregate was replaced with ECRA. ECRA should replace 20% of the natural coarse aggregate.

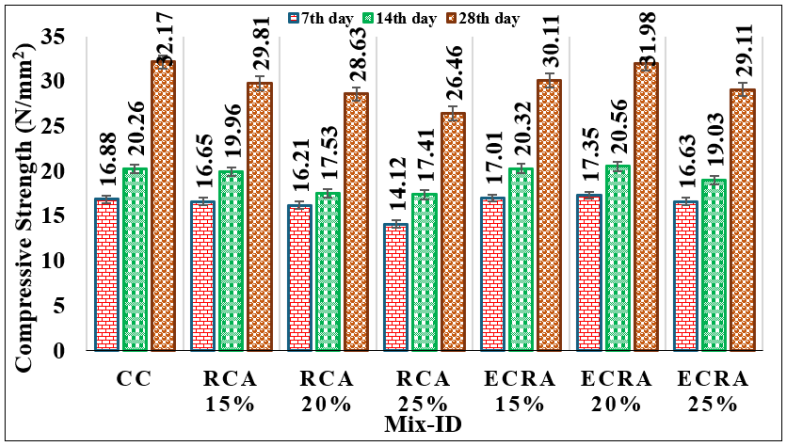

Figure 2 Compressive strength variation with days

3.2 Split tensile strength of the CC, RCA, and ECRA concrete samples

Figure 3 shows the tensile strength of the CC, RCA, and ECRA concrete splits at 7, 14, and 28 days. At 7, 14, and 28 days, the CC concrete split tensile strengths were 1.51, 2.15, and 3.35 N/mm^2. The RCA concrete split tensile strength steadily decreased, culminating at 28 days. At 28 days, 15% RCA replacement lowered the split tensile strength by 0.59%, 20% by 13.37% and 25% by 27.16%. However, the ECRA outcomes varied. On day 7, 15% of the ECRA samples had a split tensile strength of 1.52 N/mm^2, 20% had 1.49 N/mm^2 and 25% had 1.36 N/mm^2. ECRA values improved after 14 days, with 15% reaching 2.13 N/mm^2, 20% at 2.17 N/mm^2, and 25% at 1.99 N/mm^2. After 28 days, 15% ECRA achieved 3.26 N/mm^2 split tensile strength, followed by 20% at 3.42 N/mm^2 and 25% at 2.99 N/mm^2. Replacement of the natural coarse aggregate with 20% ECRA increased the TS by 2%. Aggregate coating boosts the tensile strength of concrete split with greater particle packing density and ITZ bonding. These studies confirmed the previous findings. Olofinnade and Osoata, 2023 reported that RCA coated

with metakaolin-cement is stronger than the control mix. Rajprasad and Prasanth, 2023 coated recycled aggregate with Alccofine to test its mechanical properties. Surface-coated Alccofine aggregate outperformed recyclable aggregate in terms of split tensile strength. Bharani, Gulshantaj, et al., 2021; Bharani, Rameshkumar, et al., 2021 found that e-waste partially replaced natural aggregate in concrete and enhanced the split tensile strength with 1.42%. This study found that 20% e-waste-coated recycled aggregate increased the split tensile strength by 2%.

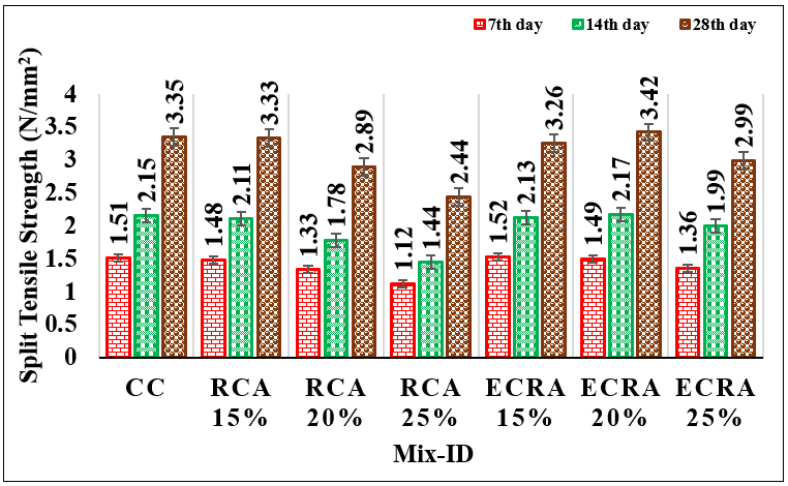

Figure 3 Split tensile strength variation with days

3.3 Flexural strength of the CC, RCA, and ERCA concrete samples

Figure 4 shows the flexural strength of the CC, RCA, and ERCA concrete at 7, 14, and 28 days. The CC concrete showed flexural strengths of 1.89, 2.55, and 3.64 N/mm^2 at 7, 14, and 28 days. The replacement of natural coarse aggregate with RCA always lowered the flexural strength, with the greatest drop at 28 days. Flexural strength decreased by 1.37%, 8.24%, and 28% with 15%, 20%, and 25% RCA, respectively, after 28 days. Low-quality RCA ITZ weakens the flexural strength. Old mortar with 25% RCA particles degrades bonding and increases porosity. Natural coarse aggregate replaced with ERCA increased flexural strength. The aggregate coating boosts flexural strength. This investigation confirmed earlier findings. Li et al., 2009 reported that pozzolanic aggregate boosts flexural strength (Bureau of Indian Standards, 2009; Li et al., 2009). Replacement of natural coarse aggregate with 15% ERCA increased the flexural strength by 0.54%. ERCA increased the flexural strength by 1.92% by replacing 20% of the natural coarse aggregate. One 25% ERCA replacement decreased flexural strength by 17.37%. High recycled content may cause ITZ degradation and microcracking.

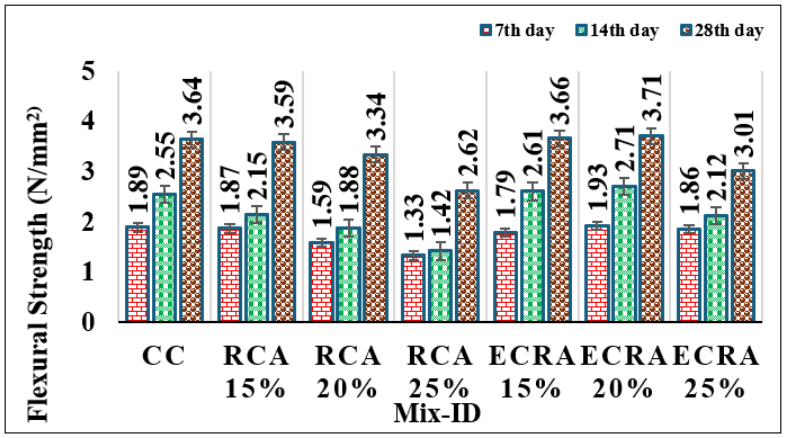

Figure 4 Flexural strength variation with days

3.4 Acid resistance of CC, RCA, and ERCA concrete samples

Table 4 demonstrates the loss of compressive strength of CC, RCA, and ECRA concrete at 7, 14, and 28 days following acidic exposure. CC mixes lose 23.0%, 17.69%, and 12.48% in compressive strength at 7, 14, and 28 days, respectively. RCA concrete loses less compressive strength than CC. The RCA15% mix lost 20.12%, 16.06%, and 10.66% of compressive strength at days 7, 14, and 28. The replacement rate increases the RCA mix compressive strength reduction. At 7, 14, and 28 days, the RCA 25% mix dropped by 14.41%, 12.49%, and 8.56%, respectively. The CC and RCA mixes lose more compressive strength than the ECRA blends. At 7, 14, and 28 days, 15% ECRA mixtures lose 20.31%, 15.21%, and 11.89% of their compressive strength. At 7, 14, and 28 days, the 20% ECRA loses 21.4%, 15.53%, and 12.2% of compressive strength. At 7, 14, and 28 days, the 25% ECRA mixtures lose 20.31%, 15.21%, and 11.89% of their compressive strength. CC and RCA lose more compressive strength than ECRA. The durable e-waste coating may densify the microstructure and reduce permeability, thereby enhancing the performance. ECRA concrete can be used by wastewater treatment plants and chemical manufacturers because of its acid resistance and lower compressive strength loss than CC and RCA. E-waste coating strengthens and prolongs the structures.

Table 4 Variation in acid attack resistance test with days

Replacement Level	Compressive strength (N/mm^2)		
	7 Days (N/mm^2)	14 Days (N/mm^2)	28 Days (N/mm^2)
CC	23.06	17.69	12.84
RCA 15%	20.12	16.06	10.06
RCA 20%	19.23	14.34	9.87
RCA 25%	14.41	12.49	8.56
ECRA 15%	20.31	15.21	11.89
ECRA 20%	21.4	15.53	12.2
ECRA 25%	20.32	13.36	9.76

3.5 Sulfate resistance of the CC, RCA, and ERCA concrete samples

Table 5 shows the reduction in CC, RCA, and ERCA concrete strength in sulfate. Concrete was tested for sulfate resistance in a sulfate solution. RCA and ERCA concrete compositions with CC and 15%, 20%, and 25% CAR were tested. Cast and cured 150 × 150 × 150 mm water specimens for 7 days. Weighing followed by washing. These specimens were then treated with 5% sodium sulfate for 7 days. The experiments measured the compressive strength loss following exposure. 7-day compressive strength loss of 18.52% for CC, 21.23% for 15% RCA, 20.94% for 20% RCA, and 15.55% for 25% RCA. The ECRA mixes lose less compressive strength than RCA mixes—22.05%, 22.56%, and 22.06% for 15%, 20%, and 25%, respectively. After 14 days, CC loses 18.52%, 15% RCA loses 17.34%, 20% loses 15.65%, and 25% RCA loses 13.65%. ECRA has lower compressive strength loss than RCA: 8.35%, 18.98%, and 18.56% for 20%, and 18.56% for 25%. RCA mixes lose 11.74%, 10.94%, and 9.87% in compressive strength at 28 days, whereas CC loses 13.89%. ECRA has a lower compressive strength loss than RCA: 12.41% for 15%, 13.05% for 20%, and 12.13% for 25%. The ECRA concrete has the lowest compressive strength loss at 7, 14, and 28 days and the highest sulfate resistance. Despite being less effective than ECRA, RCA concretes outperform CC. Concrete with ECRA and less RCA is more durable in sulfate-rich areas. ECRA concrete improves sulfate resistance in wastewater treatment facilities, coastal structures, and industrial floors with the lowest compressive strength loss.

Table 5 Sulphate attack test variation with days

Replacement Level	Compressive strength (N/mm^2)		
	7 Days (N/mm^2)	14 Days (N/mm^2)	28 Days (N/mm^2)
CC	24.03	18.52	13.89
RCA 15%	21.23	17.34	11.74
RCA 20%	20.94	15.65	10.94
RCA 25%	15.55	13.65	9.87
ECRA 15%	22.05	18.35	12.41
ECRA 20%	22.56	18.98	13.05
ECRA 25%	22.06	18.56	12.13

3.6 Water absorption rates of the CC, RCA, and ERCA concrete samples

Table 6 shows the water absorption rates of CC, RCA, and ERCA concrete. Water absorption by CC ranges from 3.68% to 6.62% after 28 days. In concrete with 15% RCA, water absorption increases from 4.2% at 7 days to 7.1% at 28 days. Concrete with 20% RCA absorbs 5.2% at day 7 and 7.5% at day 28. Concrete with 25% RCA absorbs 5.2% and 7.5% at 7 and 28 days, respectively. At 28 days, 15% of the ECRA concrete absorbs 6.8% water, up from 3.7% at 7 days. Concrete with 20% ECRA absorbs 3.4% and 6.4% at 7 and 28 days, respectively. Concrete with 25% ECRA absorbs 4.2% and 7.3% at 7 and 28 days, respectively. Although different, CC, RCA, and ECRA concrete absorb more water over time. ECRA absorbs less water than RCA because of its superior ITZ and decreased porosity. ECRA concrete has a lower water absorption rate than CC and RCA, improving aggregate bonding and water resistance in damp building applications such as basements, water tanks, and maritime constructions.

Table 6 Water Absorption measurements for M30 grade concrete at various ages

Replacement Level	Water Absorption (%)		
	7 Days (%)	14 Days (%)	28 Days (%)
CC	3.68	5.61	6.62
RCA 15%	4.2	6.1	7.1
RCA 20%	5.2	6.3	7.5
RCA 25%	6.4	7.7	9.1
ECRA 15%	3.7	5.5	6.8
ECRA 20%	3.4	5.3	6.4
ECRA 25%	4.2	5.9	7.3

3.7 Rapid chloride penetration of concrete CC, RCA, and ERCA

Sand, cement, water, and aggregates. The RCPT measures the electrical conductivity of concrete based on pore structure and solution chemistry. Chloride ion diffusion causes steel reinforcement corrosion; hence, understanding the permeability of concrete is crucial. Table 7 presents the result for the RCPT of the E-waste concrete. A water-saturated concrete specimen of 50 mm thickness and 100 mm diameter is exposed to 60 V DC for six hours in the ASTM C1202 RCPT procedure. Specialized equipment applies voltage. Some reservoirs contain 3.0% NaCl, while others contain 0.3 M NaOH. Table 7 shows the coulomb passed in CC, RCA, and ERCA concrete mixes at 7, 14, and 28 days.

ASTM C1202 links chloride ion penetration to charge passage in concrete mixes containing CC, RCA, and ERCA at 7, 14, and 28 days. Chloride ion permeability varies in M30 grade

concrete, which contains CC, RCA at 15%, 20%, and 25% replacement levels, and E-waste-coated RCA. ASTM C1202 categorizes by the total number of coulombs passed. CC chloride ion permeability drops from 1757 coulombs (Moderate) after 7 days to 1058 (low) after 28 days. However, RCA concrete has "Very Low" permeability at all ages and replacement levels, ranging from 514 coulombs at 28 days for 15% RCA to 749 at 7 days for others. At 539 and 245 coulombs after 7 days and 245 coulombs after 28 days, 15% ERCA concrete had the lowest and highest chloride ion permeability and resistance, respectively. Aggregate coating lowers coulombs of recycled aggregate concrete. These findings support Sasanipour and Aslani, 2020 observation that coating or pre-treating recycled material reduces the total coulomb passed. Kong et al., 2010 found that fly ash and slag coating recycled aggregate resists chloride ion penetration. Fly ash and slag-coated recycled aggregate contained 1140-8790 coulombs (Kong et al., 2010), whereas ERCA concrete had 245-909. Covering the recovered aggregate with e-waste powder helps. According to the study, ERCA concrete was more chloride-resistant than CC at 15% replacement. E-waste coatings increased microstructure and decreased porosity, making RCA and ERCA useful for chloride-rich concrete durability. ERCA concrete resists chloride ions, thereby benefiting coastal and marine structures. Resistance (lower coulomb passed) increases endurance and reduces maintenance and structural damage.

Table 7 Chloride permeability measurements for M30 grade concrete samples of various ages

Replacement Level	Chloride Permeability		
	7 Days	14 Days	28 Days
CC	1757	1543	1058
RCA 15%	749	617	527
RCA 20%	822	743	514
RCA 25%	941	735	609
ECRA 15%	539	418	245
ECRA 20%	812	707	658
ECRA 25%	909	738	502

3.8 XRD Analysis

XRD examination of concrete aggregates shows peaks that match the crystallographic planes in Figure 5. Minor peaks at 2θ values of 21.1, 22.15, 24.49, 27.73, 28.10, 42.11, 42.71, 50.39, 50.85, and 51.52 indicate the presence of crystalline phases in CA, including minerals from natural aggregates and electronic waste extract powder (Bahoria et al., 2018). The electronic waste extract powder adds crystalline phases to the concrete matrix, causing XRD peaks. Different chemical substances or minerals in the EW extract may have diverse XRD patterns, causing these peaks. High-abundance or larger-sized crystalline phases were indicated by high-intensity peaks at 2θ values of 26° and 61° (Islam et al., 2006). Crystallinity, size, and orientation affect the intensity of the XRD peak. The greater intensity peaks at 26° and 61° values depict that these crystallographic planes have more atoms or larger crystal domains, leading to more effective X-ray scattering and higher intensity peaks. A mineral phase with high crystallinity or greater crystal size may cause the high intensity peak at 26°, enabling more efficient XRD. The peak at 61° may be from another abundant crystalline phase or larger crystal domains. The XRD peaks in the concrete aggregate indicate crystalline phases, including those introduced by the electronic waste extract powder. High-intensity peaks at 26° and 61° indicate dominant or larger crystalline phases in the concrete matrix due to crystallinity and size.

The XRD patterns are dominated by reflections from common concrete and aggregate minerals, with the strongest peak at 26° 2θ assigned to α-quartz (SiO_2) (101), which is typical for siliceous sand/granite-derived aggregates; additional quartz reflections are consistent with

peaks near ~21.1° (100), ~42.43° (200) and ~50.4° (112), confirming quartz as a major crystalline constituent. The group of minor peaks reported between ~22.15–28.10° 2θ is most plausibly attributed to feldspar phases (albite/microcline-type silicates) commonly present in granite. However, precise (hkl) indexing for these reflections requires database matching because feldspar peak positions and indices vary by composition and symmetry. A peak expected around ~29.4° 2θ (if present in the plotted data) corresponds to calcite ($CaCO_3$) (104), and supporting calcite reflections may occur near ~42.7° (202) and ~60–61° (214); this indicates carbonation products and/or carbonate-bearing fines in the system rather than a unique e-waste signature. The reflection near ~50.85° 2θ can be assigned to portlandite, $Ca(OH)_2$ (110), representing a typical cement hydration product whose relative intensity may change with replacement level due to altered hydration/carbonation balance. Overall, the crystalline assemblage is consistent with quartz + feldspar (aggregate-derived) together with calcite and portlandite (cementitious/carbonation-derived). Any claim that e-waste powder introduces new crystalline phases should be supported by (i) XRD of the powder itself, (ii) explicit phase matching using ICDD/COD references with labeled (hkl) on the diffractograms, and (iii) Rietveld refinement to quantify phase fraction changes rather than relying on peak intensity alone.

Therefore, the principal differences between 15% and 25% are mainly expressed as changes in relative peak intensity, most notably for the dominant peaks at ~26° and ~61° 2θ, which correspond to the most abundant and/or more crystalline phases in the matrix. Since peak intensity is governed by crystallinity, crystal size, and preferred orientation (in addition to phase fraction), the observed intensity variations with replacement level are best interpreted as shifts in the relative contribution/texture of existing mineral phases rather than formation of new phases. The diffraction maxima in the 2θ range shown were indexed according to the cubic fluorite-type structure's characteristic reflection sequence (space group Fm-3m). Accordingly, the intense peak observed at approximately 29°–30° was assigned to the (111) plane, followed by the weaker contribution around 34°–36° corresponding to the (200) reflection. The mid-angle peak located near 50° was indexed as (220), whereas the dominant high-angle peak at ~59–60° was attributed to the (311) reflection. A further peak/shoulder appearing in the vicinity of 62°–63° was indexed as (222). Any additional minor features at lower angles that do not follow the fluorite reflection sequence are tentatively attributed to trace secondary phases and/or background effects; definitive assignment of those features would require the measurement wavelength (e.g., Cu Kα) and the targeted phase identity for comparison with standard reference patterns.

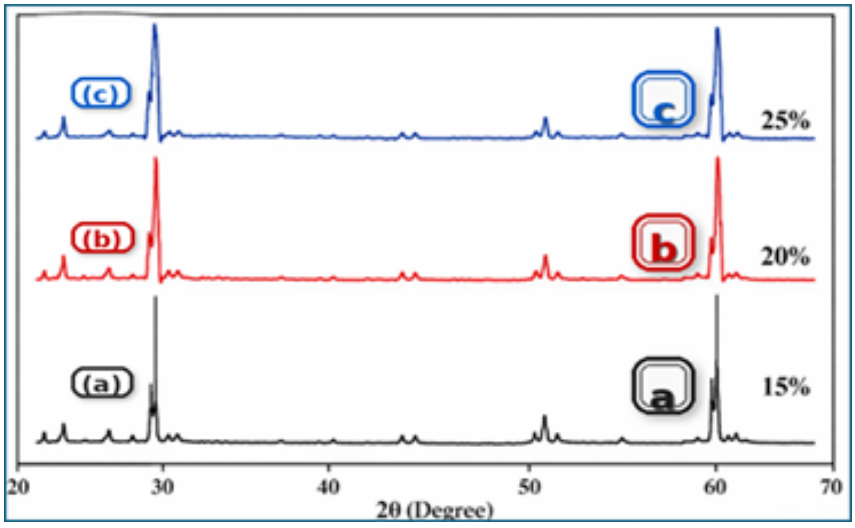

Figure 5 XRD patterns of the prepared concrete incorporating e-waste powder–coated recycled concrete aggregate (ECRA) a) 15% ECRA (b) 20% ECRA (c) 25% ECRA

3.9 SEM Analysis

Figure 6 compares the cross-sectional SEM images of normal concrete with those of ECRA (Figure 6a). E-waste powder-coated recycled aggregates (ECRA) have a distinguishing texture and roughness. Better bonding and mechanical interlock between the aggregate and concrete matrix were improved by this surface texture. The e-waste coating may improve the structural performance and durability of concrete by improving its microstructure. Plain concrete lacks the roughness and textural qualities of ECRA (Figure 6b). The aggregate-cement matrix bonding on this smoother surface may alter the mechanical qualities and durability of concrete. The integration of e-waste and the concrete matrix shows a coherent particle distribution. Optimizing strength and durability requires an appropriate distribution. The union of e-waste particles and the concrete matrix shows its successful assimilation, performance improvement, and sustainability.

The SEM study of 20% E-waste concrete reveals its morphology and structural integrity, revealing its performance and sustainability. The surface roughness and characteristics in Figure 6c indicate the material texture and mechanical qualities. Construction applications require a strong, load-bearing framework, such as the one seen in this study. E-waste is properly dispersed and homogenized in the concrete matrix shown in Figure 6d. This integration is essential to improve material qualities such as strength, durability, and environmental resistance while recycling electronic trash. Surface roughness affects adhesion, friction, and wear resistance. E-waste particle integration optimizes material utilization and distribution. SEM analysis helps construction and material engineers make sustainable infrastructure decisions by characterizing the microstructure and characteristics of 20% E-waste concrete.

3.10 FTIR

Figure 7 shows the chemical bond vibrational modes in the FTIR spectra of concrete with E-waste. Hydroxyl (OH) stretching vibrations at 3843 and 3639 cm^{-1} [49] indicate moisture or hydroxyl-containing functional groups, while C-H bonds at 3741 and 2981 cm^{-1} indicate organic molecules from electronic trash (Urban and Sicakova, 2017). Peaks at 2313 and 2045 cm^{-1} indicate C≡C and C=N triple bond stretching vibrations, indicating alkynes and nitrile groups in organic molecules, respectively (Sasanipour and Aslani, 2020). These vibrational modes reveal the chemical makeup of concrete and how moisture, organic chemicals, and potentially harmful items from electronic trash affect its quality and environmental impact. These Fourier transform infrared peaks are essential for analyzing the feasibility and sustainability of electronic waste-infused concrete.

Organic elements originating from electronic waste are apparent in the peak at 1431 cm^{-1}, which is the bending vibration of C-H bonds in aliphatic hydrocarbons or organic compounds (Olofinnade and Osoata, 2023). Incorporating organic chemicals into the concrete matrix can affect its mechanical properties and long-term behavior. Silicates or silicon-based compounds may represent the peak at 997 cm^{-1}, which is the bending vibration of Si-O-Si bonds. Specific vibrational modes of chemical bonding in the materials may explain the vast range from 1211 to 821 cm^{-1} and the peak at 773 cm^{-1}. These peaks may indicate Si-O bond stretching vibrations in silicates or silicon-based compounds. Electronic waste extract powder and natural aggregates may form these chemicals. The heterogeneous materials may explain the broadening of the peaks, indicating a chemical disturbance. Silicates were indicated by the peak at 773 cm^{-1}, which may be Si-O-Si bond bending vibration. For silicates or silicon-based materials, the peak at 644 cm^{-1} is the bending vibration of Si-O bonds. Compounds may be obtained from natural aggregates and electronic waste extract powder. Silica improves the chemical composition and structural integrity of concrete, making it more durable and environmentally resistant. Electronic waste component-derived organic molecules may explain the peaks at 591, 527, and 457 cm^{-1}, which may be C-H bond bending vibrations in aliphatic hydrocarbons or organic compounds. The presence of organic compounds in the concrete matrix can affect its

mechanical properties and long-term behavior. The 15% and 25% patterns are expected to maintain the same band positions (same cementitious/silicate framework) compared to the 20% ECRA FTIR, but differ mainly in band depth (intensity) and slight broadening. Relative to 20%, the 15% curve is drawn with weaker organic-associated absorptions (shallower dips near 2981 cm^{-1} and ĩ431 cm^{-1}) and a slightly less pronounced/broader silicate region. The 25% curve is drawn with stronger organic-associated absorptions (deeper dips near ẽ981 and ĩ431 cm^{-1}) and a slightly broader/deeper main silicate/C-S-H band around ẽ97 cm^{-1}, representing increased contribution/heterogeneity at higher replacement. These vibrational modes are important for evaluating and optimizing the composition of concrete containing electronic waste for sustainable building.

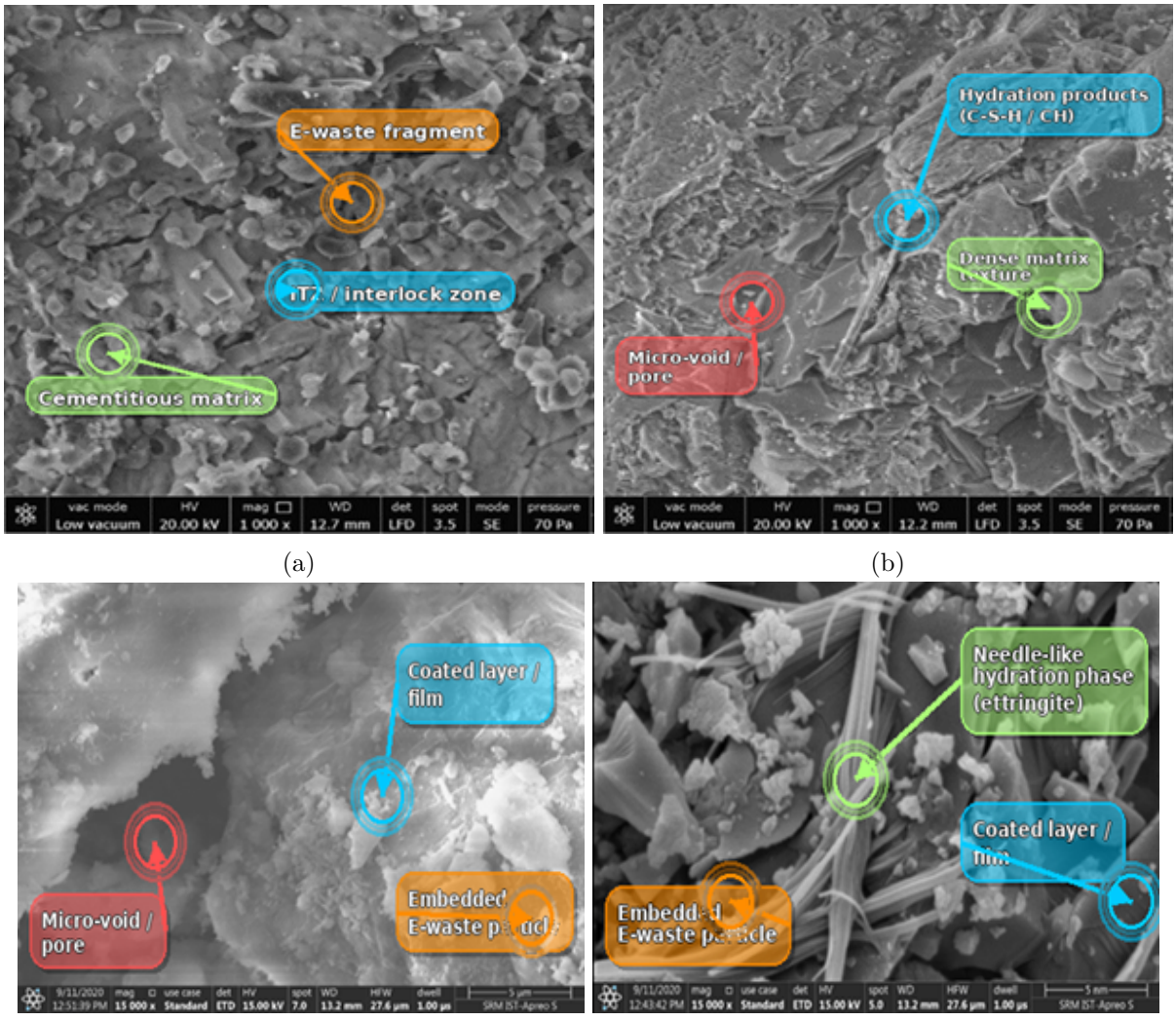

(a) (b)

(c) (d)

Figure 6 Cross-sectional SEM images of E-Waste Concrete (a) Surface of ECRA (b) Surface of Plain Concrete (c) 20% E-waste coated concrete dispersion (d) 20% E-waste coated concrete hydration

3.11 TGA and DTA results

As shown in Figure 8a, the initial mass of concrete containing 20% E-waste quickly decreased by 1.84% from 31°C to 180 °C with an onset temperature (Tonset) of 55 °C (Islam et al., 2006). Moisture evaporation causes this initial weight loss. The weight loss was 0.8% when the material decayed from 181°C to 389°C. The decomposition of organic chemicals or other volatile concrete components causes this weight loss. The material lost 0.5% of its weight at 390°C–549°C with onset at 414°C. Specific organic or inorganic concrete components may degrade, causing weight

loss. Last, the weight loss was 0.86% at 460°C–689°C (onset = 588°C). The decomposition or combustion of leftover organic materials or other thermally labile elements may have caused this weight loss. Its thermal stability has been demonstrated by its lack of breakdown beyond 700°C. The TGA study lost only 4.02% of the material, proving the durability of the concrete material. Finally, the TGA results show that the created concrete material is thermally stable at different temperatures for degradation processes such as moisture evaporation and organic and inorganic ingredient decomposition. As the temperature rises to 390°C, the DTA graph in Figure 8b shows an increase in the sample material heat flow. As the substance melts or changes phases, it absorbs energy, causing an endothermic process. Around 420 °C, the material heat flow decreases. This drop in energy absorption may indicate a localized phase shift or chemical reaction in the material. The heat flow increases to 480 °C after this decrease. Heat flow increases with time, suggesting thermal activities such as phase transitions or chemical reactions. Subsequently, the material heat flow decreases. The energy absorption rate may have decreased because of thermal processes or reactant exhaustion. The material's peak thermal capacity, or maximal energy absorption or release, has been indicated by the highest heat flow value of 2.8 mW at 380 °C. DTA analysis reveals phase transitions, chemical processes, and the thermal behavior of the sample material with increasing temperature.

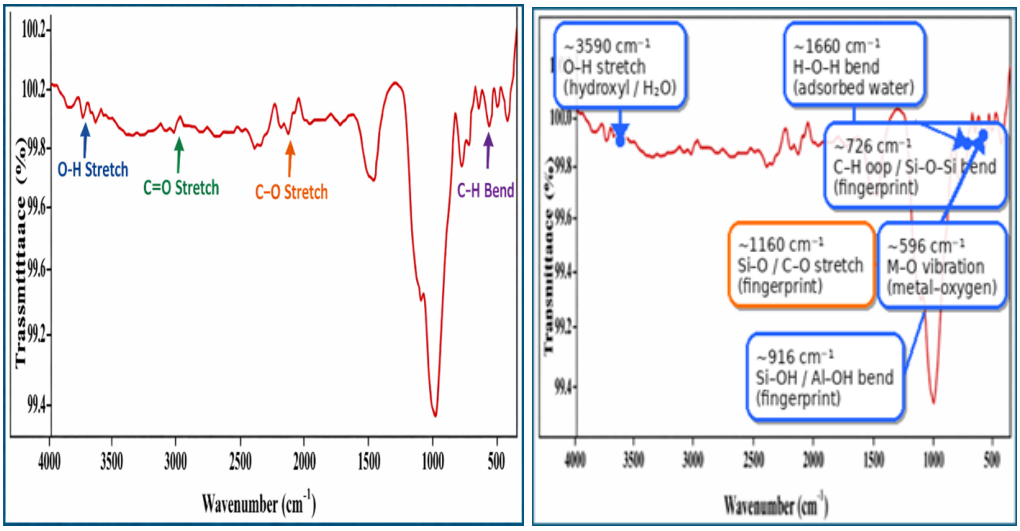

(a) (b)

Figure 7 (a) (b) FTIR of 20% ECRA

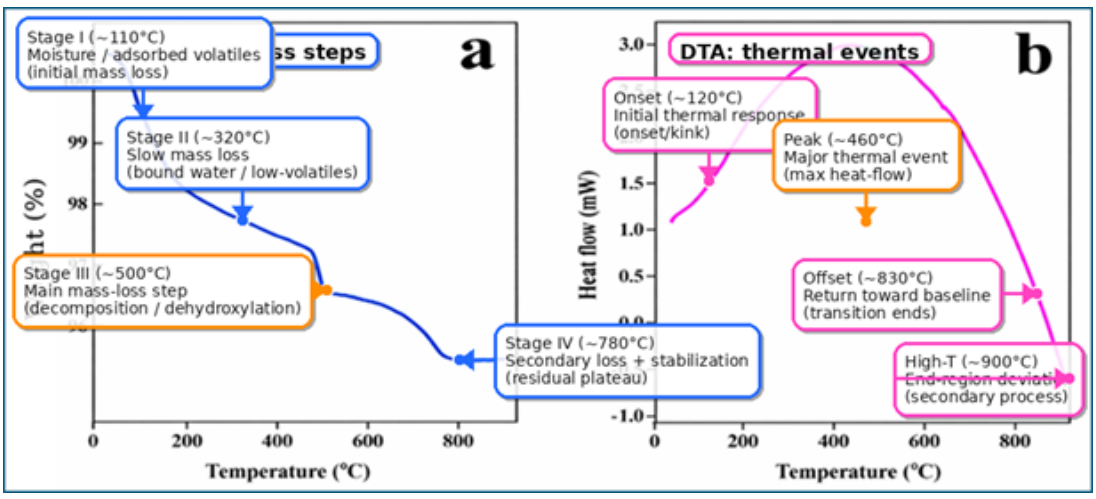

(a)

Figure 8 (a) TGA and (b) DTA of 20% ECRA

4. Conclusions

This study demonstrates that e-waste powder-coated recycled concrete aggregate (ECRA) is an effective strategy for overcoming the mechanical and durability limitations of recycled aggregate concrete while promoting sustainable waste use. Concrete containing 20% ECRA achieved a 28-day compressive strength of 31.98 MPa, which is nearly equivalent to that of the control concrete (32.17 MPa) and represents a significant recovery compared with 20% uncoated RCA, which exhibited an 11% strength reduction. At the same replacement level, the split tensile strength increased to 3.42 MPa, exceeding the control by approximately 2%, while the flexural strength improved by 1.92%, confirming enhanced aggregate–paste interfacial bonding. Durability performance also improved markedly: 28-day water absorption decreased to 6.4% for 20% ECRA compared to 7.5% for RCA, and RCPT charge values reduced to as low as 245 C, indicating very low chloride permeability relative to 1058 C for conventional concrete. Additionally, ECRA mixes exhibited reduced strength loss under acid and sulfate exposure, and TGA results showed only 4.02% mass loss up to 700 °C, confirming good thermal stability. These improvements are attributed to the e-waste coating, which densifies the recycled aggregate surface, strengthens the interfacial transition zone, and reduces porosity, as confirmed by scanning electron microscopy (SEM), X-ray diffraction (XRD), and Fourier transform infrared (FTIR) analyses. From an application perspective, the findings indicate that 20% ECRA is an optimal replacement level that balances mechanical performance, durability, and sustainability, making it suitable for structural concrete in aggressive environments such as coastal, industrial, and wastewater infrastructure. Future research should focus on the long-term durability, flexural and shear behavior of structural elements, life-cycle assessment, and large-scale field validation to facilitate the standardization and broader adoption of ECRA concrete as a high-performance, circular-economy construction material.

Acknowledgements

The authors would like to thank the Structures and Materials Research Laboratory, Prince Sultan University for their valuable support. The authors would also like to thank Prince Sultan University for paying the Article Processing Charges (APC) of this publication.

Author Contributions

J. Rajprasad: Conceptualization, Investigation, methodology, Formal Analysis, Data Curation, Writing-original draft. Musa Adamu: Data Curation, Methodology, Investigation, Writing Review & Editing. M. Mohamed Ajmal: Conceptualization, Methodology, Investigation, Writing-original draft. Yasser E. Ibrahim: Validation, Supervision, Resources, Writing Review & Editing. All authors have read and agreed to the published version of the manuscript.

Conflict of Interest

The authors declare no conflicts of interest.

References

Abrahams, C. (2017). *The Robert Gordon university, Aberdeen the Scott Sutherland school* [Doctoral dissertation]. Robert Gordon University.

Agrawal, Y., Gupta, T., Siddique, S., & Sharma, R. K. (2021). Potential of dolomite industrial waste as construction material: A review. *Innovative Infrastructure Solutions*, *6*(4), 205.

Álvarez-Pérez, J., Mesa-Lavista, M., Chavez-Gomez, J. H., & Fajardo-San Miguel, G. (2021). Experimental investigation on tensile strength of hollow concrete blocks. *Materials and Structures*, *54*(4), 164.

Bahoria, B., Parbat, D., & Nagarnaik, P. (2018). XRD analysis of natural sand, quarry dust, waste plastic (LDPE) to be used as a fine aggregate in concrete. *Materials Today: Proceedings*, *5*(1), 1432–1438. https://doi.org/10.1016/j.matpr.2017.11.230

Bharani, S., Gulshantaj, M., Rameshkumar, G., & Senthilnathan, V. (2021). Mechanical properties of concrete as partial replacement of coarse aggregate by e-waste. *IOP Conference Series: Materials Science and Engineering*, *1145*(1), 012005. https://doi.org/10.1088/1757-899X/1145/1/012005

Bharani, S., Rameshkumar, G., Manikandan, J., Balayogi, T., Gokul, M., & Bhuvanesh, D. (2021). Experimental investigation on partial replacement of steel slag and E-waste as fine and coarse aggregate. *Materials Today: Proceedings*, *37*, 3534–3537. https://doi.org/10.1016/j.matpr.2020.09.419

Bui, N. K., Satomi, T., & Takahashi, H. (2017). Improvement of mechanical properties of recycled aggregate concrete basing on a new combination method between recycled aggregate and natural aggregate. *Construction and Building Materials*, *148*, 376–385.

Bureau of Indian Standards. (1999). *Splitting tensile strength of concrete - method of test.*

Bureau of Indian Standards. (2009). *Concrete mix proportioning - guidelines.*

Bureau of Indian Standards. (2021). *Hardened concrete methods of test part 1 testing of strength of hardened concrete section 1 compressive, flexural and split tensile strength (first revision).*

de Andrade Salgado, F., & de Andrade Silva, F. (2022). Recycled aggregates from construction and demolition waste towards an application on structural concrete: A review. *Journal of Building Engineering*, *52*, 104452.

Faniran, O., & Caban, G. (1998). Minimizing waste on construction project sites. *Engineering, Construction and Architectural Management*, *5*(2), 182–188.

Gulghane, A. A., & Khandve, P. (2015). Management for construction materials and control of construction waste in construction industry: A review. *International Journal of Engineering Research and Applications*, *5*(4), 59–64.

Hino, T., Agawa, R., Moriya, Y., Nishida, M., Tsugita, Y., & Araki, T. (2009). Techniques to separate metal from waste printed circuit boards from discarded personal computers. *Journal of Material Cycles and Waste Management*, *11*(1), 42–54.

Islam, I., Chng, H., & Yap, A. (2006). X-ray diffraction analysis of mineral trioxide aggregate and Portland cement. *International Endodontic Journal*, *39*(3), 220–225. https://doi.org/10.1111/j.1365-2591.2006.01077.x

Jabbour, M., Metalssi, O. O., Quiertant, M., & Baroghel-Bouny, V. (2022). A critical review of existing test-methods for external sulfate attack. *Materials*, *15*(21), 7554. https://doi.org/10.3390/ma15217554

Janani, S., Preethi, K., Gowtham, S., & Kulanthaivel, P. (2023). A sustainable reuse of e waste as a partial replacement material for aggregate. *Materials Today: Proceedings.*

Kong, D., Lei, T., Zheng, J., Ma, C., Jiang, J., & Jiang, J. (2010). Effect and mechanism of surface-coating pozzalanics materials around aggregate on properties and ITZ microstructure of recycled aggregate concrete. *Construction and Building Materials*, *24*(5), 701–708. https://doi.org/10.1016/j.conbuildmat.2009.10.038

Kuzina, E., Cherkas, A., & Rimshin, V. (2018). Technical aspects of using composite materials for strengthening constructions. *IOP Conference Series: Materials Science and Engineering.*

Li, J., Xiao, H., & Zhou, Y. (2009). Influence of coating recycled aggregate surface with pozzolanic powder on properties of recycled aggregate concrete. *Construction and Building Materials*, *23*(3), 1287–1291. https://doi.org/10.1016/j.conbuildmat.2008.07.019

Liu, Y., Ren, P., Garcia-Troncoso, N., Mo, K. H., & Ling, T.-C. (2022). Roles of enhanced ITZ in improving the mechanical properties of concrete prepared with different types of recycled aggregates. *Journal of Building Engineering*, *60*, 105197. https://doi.org/10.1016/j.jobe.2022.105197

Lokesh Kumar, S., Binish, C., Rajprasad, J., Tabassum, S., Sadaiyandi, V., Ramaraj, S. G., Wadaan, M. A., Vatin, N. I., Govindaraju, S., & Vijayasankar, A. (2024). Synergistic fabrication, characterization, and prospective optoelectronic applications of DES grafted activated charcoal dispersed PVA films. *Polymers for Advanced Technologies*, *35*(5), e6422.

Lotfi, S., Eggimann, M., Wagner, E., Mróz, R., & Deja, J. (2015). Performance of recycled aggregate concrete based on a new concrete recycling technology. *Construction and Building Materials*, *95*, 243–256. https://doi.org/10.1016/j.conbuildmat.2015.07.021

Luhar, S., & Luhar, I. (2019). Potential application of E-wastes in construction industry: A review. *Construction and Building Materials*, *203*, 222–240.

Mangialardo, A., & Micelli, E. (2017). Rethinking the construction industry under the circular economy: Principles and case studies. *International Conference on Smart and Sustainable Planning for Cities and Regions*.

Marimuthu, V., & Ramasamy, A. (2024). Mechanical characteristics of waste-printed circuit board-reinforced concrete with silica fume and prediction modelling using ANN. *Environmental Science and Pollution Research*, *31*(19), 28474–28493.

Masud, M. H., Mourshed, M., Mahjabeen, M., Ananno, A. A., & Dabnichki, P. (2022). Global electronic waste management: Current status and way forward. In *Paradigm shift in e-waste management* (pp. 9–47).

McNeil, K., & Kang, T. H.-K. (2013). Recycled concrete aggregates: A review. *International Journal of Concrete Structures and Materials*, *7*(1), 61–69.

Muthupriya, P., & Kumar, B. V. (2021). Experimental investigation on concrete with E-waste-A way to minimize solid waste deposition. *Nature Environment and Pollution Technology*, *20*(3), 1185–1191.

Needhidasan, S., Ramesh, B., & Prabu, S. J. R. (2020). Experimental study on use of E-waste plastics as coarse aggregate in concrete with manufactured sand. *Materials Today: Proceedings*, *22*, 715–721.

Niu, B., E, S., Song, Q., Xu, Z., Han, B., & Qin, Y. (2024). Physicochemical reactions in e-waste recycling. *Nature Reviews Chemistry*, *8*(8), 569–586.

Olofinnade, O. M., & Osoata, O. P. (2023). Performance assessment of mechanical properties of green normal strength concrete produced with metakaolin-cement coated recycled concrete aggregate for sustainable construction. *Construction and Building Materials*, *407*, 133508. https://doi.org/10.1016/j.conbuildmat.2023.133508

Perkins, D. N., Drisse, M.-N. B., Nxele, T., & Sly, P. D. (2014). E-waste: A global hazard. *Annals of Global Health*, *80*(4), 286–295.

Rajprasad, J., & Prasanth, J. (2023). Evaluation of surface-coated recycled coarse aggregate in concrete using alccofine. *International Conference on Civil Engineering Innovative Development in Engineering Advances*, 89–102. https://doi.org/10.1007/978-981-99-6233-4_9

Raman, J. V. M., & Ramasamy, V. (2021). Various treatment techniques involved to enhance the recycled coarse aggregate in concrete: A review. *Materials Today: Proceedings*, *45*, 6356–6363. https://doi.org/10.1016/j.matpr.2020.10.935

Roy, H., Rahman, T. U., Suhan, M. B. K., Al-Mamun, M. R., Haque, S., & Islam, M. S. (2022). A comprehensive review on hazardous aspects and management strategies of electronic waste: Bangladesh perspectives. *Heliyon*, *8*(7).

Sangamesha, M., Kumar, S. L., Pushpalatha, K., Nithin, K., & Ranganatha, V. L. (2023). Influence of copper selenide nanoparticles on structural, optical and opto-electronic properties of polyinylalcohol/copper selenide composites. *AIP Conference Proceedings*.

Sasanipour, H., & Aslani, F. (2020). Durability assessment of concrete containing surface pretreated coarse recycled concrete aggregates. *Construction and Building Materials*, *264*, 120203. https://doi.org/10.1016/j.conbuildmat.2020.120203

Shahane, H. A., & Bhosale, S. S. (2021). E-Waste plastic powder modified bitumen: Rheological properties and performance study of bituminous concrete. *Road Materials and Pavement Design*, *22*(3), 682–702.

Singh, H., & Siddique, R. (2025). A detailed insight into rate of water absorption of concrete: Experimental and modelling approach. *Expert Systems with Applications*, *267*, 126209.

Szałatkiewicz, J. (2014). The amount of PCBs in WEEE. *Polish Journal of Environmental Studies*, *23*(6), 2365–2369.

Ullah, S., Qureshi, M. I., Joyklad, P., Suparp, S., Hussain, Q., Chaiyasarn, K., & Yooprasertchai, E. (2022). Effect of partial replacement of E-waste as a fine aggregate on compressive behavior of concrete specimens having different geometry with and without CFRP confinement. *Journal of Building Engineering*, *50*, 104151.

Urban, K., & Sicakova, A. (2017). The influence of kind of coating additive on the compressive strength of RCA-based concrete prepared by triple-mixing method. *IOP Conference Series: Earth and Environmental Science*. https://doi.org/10.1088/1755-1315/92/1/012069

Wang, R., Jin, P., Ding, Z., & Zhang, W. (2021). Surface modification of recycled coarse aggregate based on Microbial Induced Carbonate Precipitation. *Journal of Cleaner Production*, *328*, 129537.

Wu, B., Liu, C., & Wu, Y. (2014). Compressive behaviors of cylindrical concrete specimens made of demolished concrete blocks and fresh concrete. *Construction and Building Materials*, *53*, 118–130.

Xiao, R., Zhang, M., Zhong, J., Baumgardner, G. L., & Huang, B. (2025). Waste plastic powder coating on acidic aggregates: A new hydrophobic coating technology to build moisture-resistant asphalt mixtures. *Transportation Research Record*, *2679*(1), 992–1005.

Yamane, L. H., de Moraes, V. T., Espinosa, D. C. R., & Tenório, J. A. S. (2011). Recycling of WEEE: Characterization of spent printed circuit boards from mobile phones and computers. *Waste Management*, *31*(12), 2553–2558.

Zhu, P., Hao, Y., Liu, H., Wang, X., & Gu, L. (2020). Durability evaluation of recycled aggregate concrete in a complex environment. *Journal of Cleaner Production*, *273*, 122569.